

Oriented Protein Immobilization using Covalent and Noncovalent Chemistry on a Thiol-Reactive Self-Reporting Surface

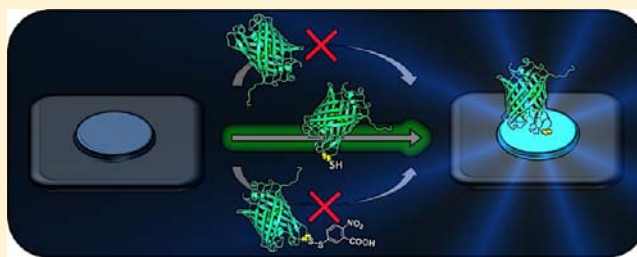
Dorothee Wasserberg,^{†,‡,§} Carlo Nicosia,^{†,§} Eldrich E. Tromp,^{†,‡} Vinod Subramaniam,^{*,‡} Jurriaan Huskens,^{*,†} and Pascal Jonkheijm^{*,†}

[†]Molecular Nanofabrication Group, MESA⁺ Institute for Nanotechnology, Department of Science and Technology, University of Twente, 7500 AE, Enschede, Netherlands

[‡]Nanobiophysics Group, MESA⁺ Institute for Nanotechnology and MIRA Institute for Biomedical Technology and Technical Medicine, Department of Science and Technology, University of Twente, 7500 AE, Enschede, Netherlands

S Supporting Information

ABSTRACT: We report the fabrication of a patterned protein array using three orthogonal methods of immobilization that are detected exploiting a fluorogenic surface. Upon reaction of thiols, the fluorogenic tether reports the bond formation by an instantaneous rise in (blue) fluorescence intensity providing a means to visualize the immobilization even of nonfluorescent biomolecules. First, the covalent, oriented immobilization of a visible fluorescent protein (TFP) modified to display a single cysteine residue was detected. Colocalization of the fluorescence of the immobilized TFP and the fluorogenic group provided a direct tool to distinguish covalent bond formation from physisorption of proteins. Subsequent orthogonal immobilization of thiol-functionalized biomolecules could be conveniently detected by fluorescence microscopy using the fluorogenic surface. A thiol-modified nitrilotriacetate ligand was immobilized for binding of hexahistidine-tagged red-fluorescing TagRFP, while an appropriately modified biotin was immobilized for binding of Cy5-labeled streptavidin.



1. INTRODUCTION

Convenient ways to link proteins to predefined locations on molecular and supramolecular reactive surfaces are of great importance for bottom-up engineering in nanotechnology and life sciences.¹ Site-specific chemical strategies, as opposed to random attachment, provide precise control over immobilizing proteins in homogeneously oriented layers and yield improved performance of protein biochips.^{2–4} For the immobilization of structurally sensitive proteins, chemical reactions with high specificity toward the protein of interest, mild reaction conditions compatible with physiological conditions, and rapid and quantitative conversion are essential.² Among the bioanalytical platforms under development, interfaces with multiple proteins on a single surface with predetermined density, spacing, and orientation have attracted much attention.⁵ Promising progress has been reported on developing multifunctional protein surfaces using diverse surface-bound orthogonal chemical functionalities for subsequent protein attachment via covalent and noncovalent chemistry. To achieve spatial surface patterning of orthogonal chemical groups, elegant techniques have been developed,⁶ including photolithography,⁷ spot arraying,⁸ electron-beam lithography,⁹ dip-pen and other probe lithographies,¹⁰ and imprint lithography¹¹ as well as microcontact printing (μ CP).¹² While a few of the above-mentioned spatially multifunctionalized surfaces are documented in the literature, where site-specific protein attachment has been realized, only a small number are shown

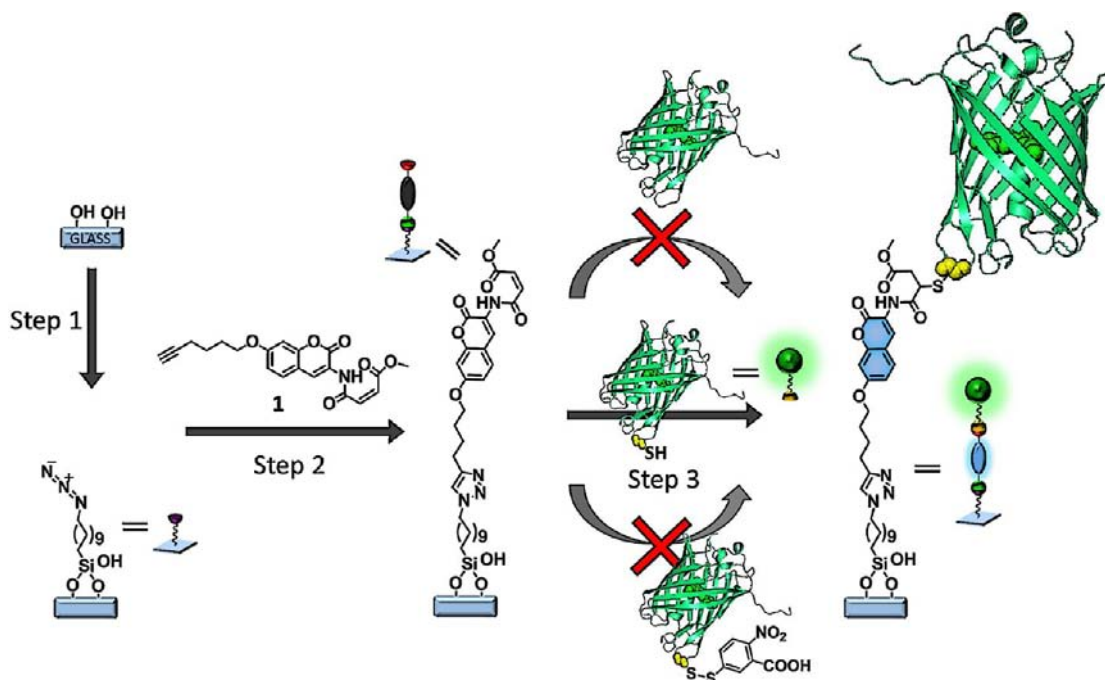
to combine orthogonal covalent with noncovalent protein immobilization strategies. Employing such multifunctional protein(-binding) surfaces is attractive to achieve differentiated responsive biomimetic functions.¹³ Recently, Velders and co-workers demonstrated the selectivity and specificity of orthogonal covalent and noncovalent functionalization for small molecules. In their work bifunctional alkyne-cyclodextrin patterned surfaces were prepared via reactive μ CP.¹⁴ Microcontact printing is a versatile surface patterning method that has been exploited for the immobilization of many different molecules by inducing different types of reactions.¹⁵ In a very recent example, Ravoo and co-workers fabricated tetra-functional chemical patterns on silicon oxide by consecutive reactive prints of heterofunctional linkers,^{12d} each with a ligand attached, displaying excellent biomolecular specificity.^{12d}

Here, we employ our self-reporting thiol-reactive fluorogenic platform¹⁶ to fabricate an interface with covalently and noncovalently bound proteins. Oriented protein immobilization can be conveniently achieved if the protein possesses a single accessible, reactive cysteine (Cys), which is the only naturally occurring amino acid containing a thiol group in its side chain, and whose relative abundance in proteins is rather small (<1%). Thiols have a pK_a of around 8.5 and are sufficiently nucleophilic at pH 7. When Cys residues are introduced into a protein

Received: October 16, 2012

Published: February 4, 2013

Scheme 1. Schematic Representation of the Surface Functionalization by Reactive μ CP of **1** (step 2) on an Azide Monolayer (from step 1), Followed by Immobilization of a Single-Cysteine-Containing Mutant of TFP (G^{174C} TFP, step 3) Reported by the Fluorogenic Reaction of **1**, (step 3, center)^a



^aSchematic representation of the protein structures: control cysteine-free TFP (step 3, top), G^{174C} TFP (step 3, center), and blocked G^{174C} TFP after derivatization with Ellman's reagent (step 3, bottom).

through site-specific mutation of, for example, Ser or Ala residues, preferably in a remote solvent-accessible epitope of the protein, the specific reaction of an engineered cysteine moiety with our fluorogenic maleimide-terminated monolayers can be conveniently detected. Colocalization of the fluorescence of the immobilized protein and of the fluorogenic group provides a direct tool to distinguish covalent bond formation from physisorption. Equally, the orthogonal attachment of subsequent immobilization steps of thiol-functionalized biomolecules can be identified via this colocalization of fluorescence signatures.

2. RESULTS AND DISCUSSION

2.1. Direct Oriented Immobilization of Cysteine-Modified Proteins from Solution. Visible fluorescent proteins were used as model proteins in this study as their fluorescence serves as an intrinsic probe for their structural integrity upon immobilization, since their fluorescence characteristics are highly sensitive to even minute changes in their native structure.¹⁷ For the preparation of micropatterned protein surfaces, glass slides were first modified with an azide-terminated monolayer (Scheme 1, step 1).¹⁸ Then, a 1 h single reactive μ CP step (Scheme 1, step 2), by the Huisgen 1,3-dipolar cycloaddition,¹⁹ was performed employing an oxidized poly(dimethylsiloxane) (PDMS) stamp inked with a solution of alkyne-functionalized fluorogenic coumarin **1** (Scheme 1), $\text{Cu(I)}(\text{CH}_3\text{CN})_4\text{PF}_6$, and tris[(1-benzyl-1H-1,2,3-triazol-4-yl)methyl] amine (TBTA).

The presence of a methyl-4-oxo-2-butenate group adjacent to the coumarin allows reaction with thiols and quenches the coumarin emission prior to reaction with such thiols.^{16,20} Owing to this quenching, upon printing of **1**, the fluorescence of the pattern was almost indistinguishable from the back-

ground (Figure 1a).¹⁶ Subsequently, onto this self-reporting platform the covalent immobilization of thiol-containing compounds was performed by means of the fluorogenic Michael addition to the methyl-4-oxo-2-butenate moiety of **1** (Scheme 1, step 3, center).

To establish the method for the direct covalent immobilization on the self-reporting surface of a cysteine-modified protein (Scheme 1), a single-cysteine-containing mutant of a monomeric variant of *Clavularia* cyan fluorescent protein, **mTFP1**,²¹ was recombinantly expressed and purified [see Supporting Information (SI) for details]. **mTFP1** was modified to contain no hexa-histidine (His_6)-tags and, additionally, was site-selectively mutated to introduce a single cysteine group at the 174 position, which is located in a flexible loop on top of the β -barrel of the fluorescent protein, yielding G^{174C} TFP. To probe the applicability of the direct protein immobilization, a 20 μM phosphate buffered solution (pH 7.5) of G^{174C} TFP was used for overnight incubation of substrates patterned with **1**. As control for the specificity of the immobilization reaction, the cysteine-free mutant, TFP, was used at even higher concentrations (40 μM) but otherwise identical conditions. After overnight incubation fluorescence micrographs showed protein patterns colocalized on the fluorescent coumarin patterns only in the case of G^{174C} TFP (Figure 1c,d), whereas no enhancement of fluorescence of the fluorogenic coumarin or any other part of the pattern in the case of TFP (Figure 1a,b) could be observed, proving that the reaction indeed proceeds exclusively with thiol-containing proteins.

The thus generated signaling platform is indeed so specific to thiol moieties that it may become a valuable tool for the identification of the redox state of cysteines, which are important to the folding and stability of some proteins that are part of various signaling pathways.²² To prove the ability of

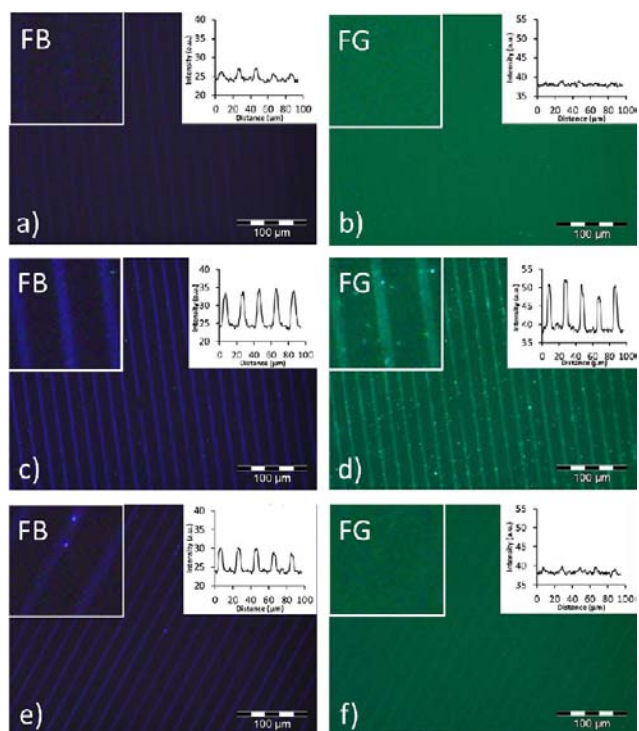


Figure 1. (a–f) Fluorescence micrographs (insets: corresponding intensity profiles) of substrates patterned with **1**, after overnight incubation with: (a,b) 40 μM TFP; (c,d) 20 μM G^{174C} TFP; and (e,f) 30 μM G^{174C} TFP after reaction with Ellman's reagent. FB/FG refer to blue (monitoring coumarin) and green (monitoring TFP) fluorescence channels, respectively.

our platform to selectively distinguish between thiols and disulfides, a series of substrates were patterned with fluorogenic coumarin **1** and subsequently incubated with TFP, G^{174C} TFP, or a disulfide conjugate of G^{174C} TFP. To yield such a disulfide conjugate of G^{174C} TFP, a 20 μM solution of G^{174C} TFP and, as a control, cysteine-free TFP were reacted with an excess of Ellman's reagent²³ (see SI). After overnight incubation of G^{174C} TFP, TFP, and the reaction product of G^{174C} TFP with

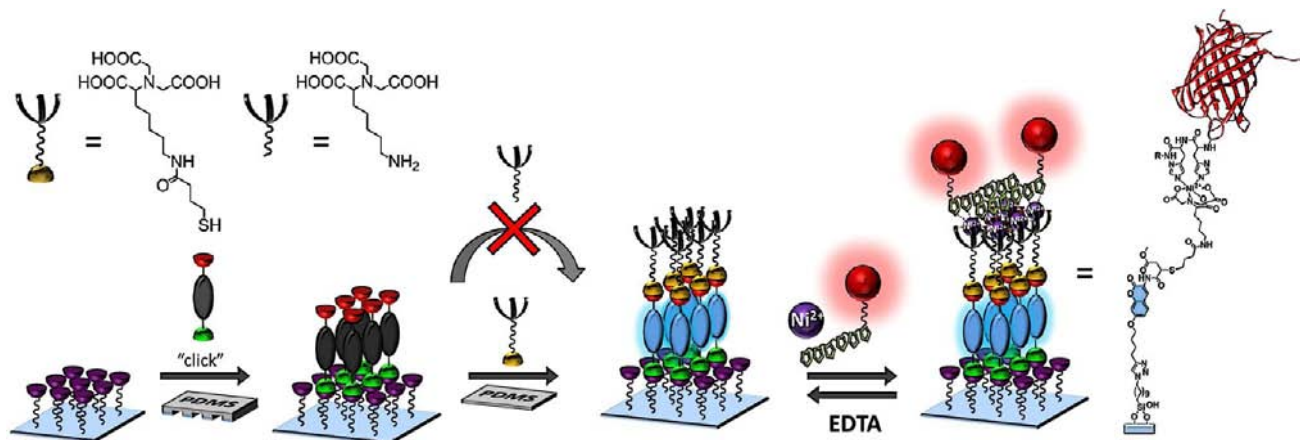
Ellman's reagent on slides, which were patterned in lines with **1**, significant fluorescent (protein) patterns could only be observed in the case of unreacted G^{174C} TFP (Figure 1d). However, upon incubation with the disulfide conjugate of G^{174C} TFP, a very weak fluorescent pattern could be observed (Figure 1f) a modest increase of blue fluorescence from the coumarin lines was detected (Figure 1e). This is probably due to the reaction with residual free thiol-containing byproducts from the disulfide formation with Ellman's reagent.

These results show that only free thiol containing G^{174C} TFP is immobilized but not its disulfide conjugate. The above series of experiments prove that: (a) thiol-containing proteins can be directly immobilized on fluorogenic coumarin patterns; (b) direct protein immobilization gives rise to the self-reporting blue fluorescence signal of the thiol-addition product of the tethered coumarin; (c) immobilization from a solution of G^{174C} TFP results in colocalized patterns of protein and fluorogenic coumarin; and (d) immobilization of G^{174C} TFP on fluorogenic coumarin is chemo-selective, i.e., thiol-containing G^{174C} TFP but neither thiol-free TFP nor G^{174C} TFP-disulfide conjugates are immobilized.

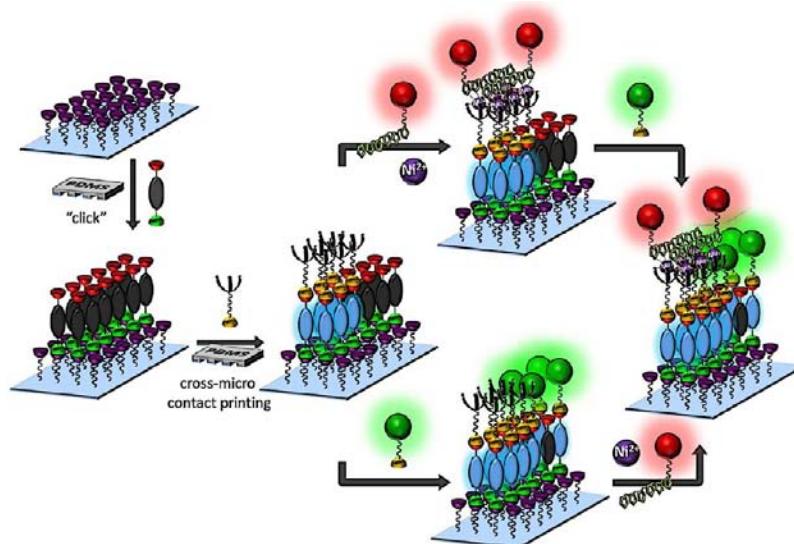
2.2. Supramolecular Oriented Immobilization of His₆-Tagged Proteins in Distinct Patterns. With the goal of fabricating a multifunctional patterned surface that allows for oriented covalent and noncovalent protein immobilization, we decided to make use of the Ni(II)-nitrilotriacetic acid (NiNTA)/His₆-tag technology. To this end, cross-patterns were fabricated by performing a second reactive μCP step of thiol-NTA perpendicularly oriented with respect to the line-patterns of **1** (Scheme 2). This printing step should result in NTA-functionalized areas adjacent to areas of unreacted, 'dark', coumarins to be used for the direct covalent immobilization of cysteine-modified proteins from solution in a subsequent step (Scheme 3).

In contrast to our previous work where thiolated molecules,¹⁶ a pentapeptide,¹⁶ and a protein (*vide supra*) were immobilized from solution, the viability of reactive μCP of thiol-containing compounds on prepatterned fluorogenic coumarin was tested. To this end, cysteine was selected for immobilization via reactive μCP on our self-reporting platform.

Scheme 2. Schematic Representation of the Procedure of the Supramolecular Protein Immobilization by Reactive μCP of **1 on an Azide Monolayer, Followed by Immobilization of a Thiol-NTA Reported by the Fluorogenic Reaction and Subsequent Colocalization of His₆-¹⁴TagRFP-His₆ Immobilized via NiNTA/His₆ Interactions^a**



^aThe molecular structure of the NiNTA/His₆ complex represents one of the possible species formed upon interactions of a His₆-tag with a single NiNTA unit.

Scheme 3. Schematic Representation of the Fabrication of a Dual Protein Array^a

^a(Step 1) Surface functionalization by reactive μ CP of **1** on an azide monolayer, followed by (step 2) immobilization of thiol-NTA by cross- μ CP. (Step 3) Subsequent immobilization of $\text{His}_6\text{-}^{14}\text{TagRFP-His}_6\text{:Ni}^{2+}$ on the NTA pattern (upper route, Figures S4 and S5) and consecutive immobilization of cysteine-containing $^{G174C}\text{TFP}$ from solution on the rest of the pattern of as yet unreacted coumarin tether or, alternatively, *vice versa* (step 3, lower route, Figure 3) the immobilization of $^{G174C}\text{TFP}$ with the consecutive immobilization of $\text{His}_6\text{-}^{14}\text{TagRFP-His}_6\text{:Ni}^{2+}$.

After a flat PDMS stamp was inked with a 10 mM cysteine solution in PBS for 30 min and dried in a flow of nitrogen, the stamp was brought into conformal contact with the self-reporting coumarin-patterned substrate for 10 min. The fluorescence microscopy characterization of the monolayers showed a very weak signal for the unreacted fluorogenic moiety before and a strong blue fluorescence emission after reactive μ CP of cysteine (Figure S1). Due to immobilization via reactive μ CP, the required sample volume and concentration were much reduced compared to that required for the previously reported immobilization from solution.¹⁶ From the fluorescence micrographs it is obvious that after performing two reactive μ CP steps, a Huisgen 1,3-dipolar cycloaddition of **1** on the azide-functionalized monolayer followed by a fluorogenic Michael addition on patterns of **1**, the cysteine-printed areas of the fluorogenic coumarin pattern had indeed increased in fluorescence intensity. This demonstrates the viability of using reactive μ CP to immobilize thiols on our fluorogenic platform.

Then, following the same procedure as described above for cysteine, thiol-NTA was immobilized via reactive μ CP (using a flat stamp) on fluorogenic coumarin reporter patterns (Figure 2). After printing, the blue fluorescent coumarin pattern was clearly visible (Figure 2a), confirming the successful immobilization of thiol-NTA. Subsequently, a variant $\text{His}_6\text{-}^{14}\text{TagRFP-His}_6$ (SI) of monomeric red fluorescent protein, derived from *Entacmaea quadricolor*, TagRFP,²⁴ carrying His₆-tags at both N- and C-terminus was used for supramolecular immobilization on the NTA-patterns. The NTA-patterned sample was incubated with a solution of 1 μM $\text{His}_6\text{-}^{14}\text{TagRFP-His}_6$ and NiCl_2 in a 1:2 ratio for 30 min, washed for 1 h, dried, and imaged using fluorescence microscopy. The fluorescence characterization (Figure 2c,d) shows a perfect colocalization of the covalently attached NTA (determined via coumarin) and the assembled fluorescent protein. Then, the sample was shortly immersed in a 10 mM ethylene diamine tetraacetic acid (EDTA) solution in order to remove the protein from the NTA monolayer via competitive complexation of Ni^{2+} ions by EDTA. This resulted

in the retention of the immobilized NTA as seen by the remaining signal from the coumarin (Figure 2e) and, at the same time, a substantial loss of the red fluorescence intensity (Figure 2f) indicating desorption of the protein. This demonstrates the reversibility and specificity of the $\text{His}_6\text{-}^{14}\text{TagRFP-His}_6$ interaction with the NTA-patterns. The selectivity of the immobilization for thiols was further confirmed using an amino-NTA, lacking a thiol group (Scheme 2). After printing the amino-NTA on fluorogenic coumarin patterns using a flat stamp, negligible enhancement of fluorescence was observed (Figure 2g). Upon subsequent incubation with $\text{His}_6\text{-}^{14}\text{TagRFP-His}_6$ and NiCl_2 , the slight increase in red fluorescent patterns (Figure 2h) indicates that hardly any nonspecific interactions occur between the protein and the NTA-free surface.

From this series of experiments we concluded that: (a) thiol-NTA is site-selectively immobilized on our fluorogenic platform following a reactive μ CP approach; (b) immobilization gives rise to the self-reporting blue fluorescence signal of the thiol addition product of coumarin upon reactive μ CP; (c) immobilization from a solution of $\text{His}_6\text{-}^{14}\text{TagRFP-His}_6$ with NiCl_2 results in colocalized patterns of protein and NTA; (d) immobilization of $\text{His}_6\text{-}^{14}\text{TagRFP-His}_6$ in the presence of Ni^{2+} ions on NTA patterns on fluorogenic coumarin is selective and reversible.

2.3. Protein Arrays through Oriented Covalent and Noncovalent Immobilization. To fabricate arrays using covalent and noncovalent immobilization of two different proteins, we next set out to show immobilization of NTA ligands only on parts of the fluorogenic coumarin patterns (Scheme 3). To this end, a line-patterned PDMS stamp inked with thiol-NTA solution was cross-microcontact printed on a substrate prepatterned with lines of **1** so that the two line patterns were oriented perpendicular to each other. This resulted in NTA-functionalized squares at the locations where the two patterns overlap, while the remainder of the lines functionalized with the fluorogenic unit **1** remained unreacted

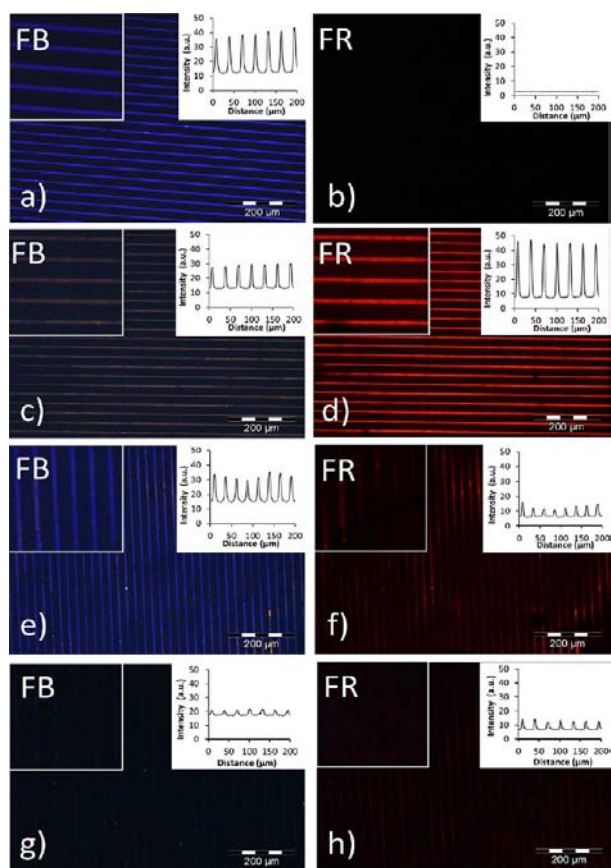


Figure 2. Fluorescence micrographs (insets: corresponding intensity profiles): (a,b) after printing of thiol-NTA with a flat PDMS stamp on a substrate patterned with compound **1**; (c,d) after incubation of the previous substrate in $\text{His}_6\text{-}^{14}\text{TagRFP-His}_6\text{:Ni}^{2+}$ (1:2) in PBS; (e,f) after immersion in 10 mM EDTA in PBS (different substrate); (g) after printing amino-NTA with a flat PDMS stamp; and (h) after incubation of this substrate in $\text{His}_6\text{-}^{14}\text{TagRFP-His}_6\text{:Ni}^{2+}$ in PBS. FB/FR refer to blue (monitoring coumarin) and red (monitoring TagRFP) channels, respectively.

and still thiol-reactive. Upon incubation of such a substrate with $1 \mu\text{M}$ $\text{His}_6\text{-}^{14}\text{TagRFP-His}_6\text{:Ni}^{2+}$ (1:2 ratio) in PBS, the selective colocalization of protein on the NTA-functionalized squares was observed (Figures S2 and S3). To test the ability to immobilize $\text{G}^{174\text{C}}\text{TFP}$ onto the remaining 'dark' areas of the as yet unreacted lines of fluorogenic coumarin and the His_6 -tagged protein on the NTA-functionalized areas of the same substrate, two procedures comprising two consecutive immobilization steps were carried out (Scheme 3). In one procedure the His_6 -tagged proteins were supramolecularly immobilized on the NTA patterns prior to the direct covalent immobilization of the

cysteine-containing variant $\text{G}^{174\text{C}}\text{TFP}$ on the as yet unreacted fluorogenic patterns (Scheme 3, upper route), while in the other procedure the order of the two immobilization steps was reversed (Scheme 3, lower route). Both routes lead to the same result: dual protein patterns of oriented, noncovalently immobilized $\text{His}_6\text{-}^{14}\text{TagRFP-His}_6$ on NTA and covalently immobilized $\text{G}^{174\text{C}}\text{TFP}$ on the non-NTA functionalized coumarin, respectively.

In detail, following the lower route in Scheme 3, a square cross-microcontact printed substrate of thiol-NTA on patterns of **1** (Figure 3a) was incubated overnight with a $20 \mu\text{M}$ solution of $\text{G}^{174\text{C}}\text{TFP}$. After washing, 1 h incubating with a solution of $1 \mu\text{M}$ $\text{His}_6\text{-}^{14}\text{TagRFP-His}_6\text{:Ni}^{2+}$ (1:2 ratio), and finally washing and drying in a flow of nitrogen, a series of fluorescence micrographs were recorded using different filters (Figure 3b–d). As can be concluded from the merged fluorescence images (Figure 3e), squares of $\text{His}_6\text{-}^{14}\text{TagRFP-His}_6\text{:Ni}^{2+}$ are localized on parts of the blue-fluorescent coumarin lines complementary to where $\text{G}^{174\text{C}}\text{TFP}$ is localized. Furthermore, the coumarin lines are fully functionalized, as they show highly intense blue fluorescence along their entire lengths (Figure 3b). Remarkably, there seems to be a systematically higher intensity in the blue coumarin fluorescence colocalized exactly at the squares of cross-microcontact printed thiol-NTA, while the rectangular parts of the coumarin lines in-between, functionalized with $\text{G}^{174\text{C}}\text{TFP}$, consistently show a lower blue (coumarin) fluorescence intensity. Since our self-reporting platform reflects bond formation, we correlate this observation to a higher surface coverage in the case of the small molecule, thiol-NTA, in comparison to the much larger protein (Figure S7). When the order of incubation was reversed, following the upper route in Scheme 3, i.e., first $\text{His}_6\text{-}^{14}\text{TagRFP-His}_6$ and then $\text{G}^{174\text{C}}\text{TFP}$, equally specific complementary patterns were observed (Figure S5), with similar fluorescence intensity ratios in both cases. It should be mentioned that calibration experiments on protein fluorescence intensities of immobilized $\text{His}_6\text{-}^{14}\text{TagRFP-His}_6$ and $\text{G}^{174\text{C}}\text{TFP}$ indicate similar coverages for both proteins of $\sim 30\%$ (Figure S7 and S8).

With this series of experiments, we show that: (a) NiNTA and thiol-sensitive coumarin tethers can be used to orthogonally immobilize two different proteins, one containing His_6 -tags and one containing a free cysteine regardless of the order in which the proteins are immobilized; (b) the immobilization strategies are orthogonal and (chemo)-selective; and (c) the fluorogenic tether acts as fluorescent reporter for the immobilization of thiols, while (d) a correlation between fluorescence intensity and coverage of bound thiols can be detected.

After optimizing the conditions for fabricating a bifunctional surface for dual protein patterns, the use of the residual azide

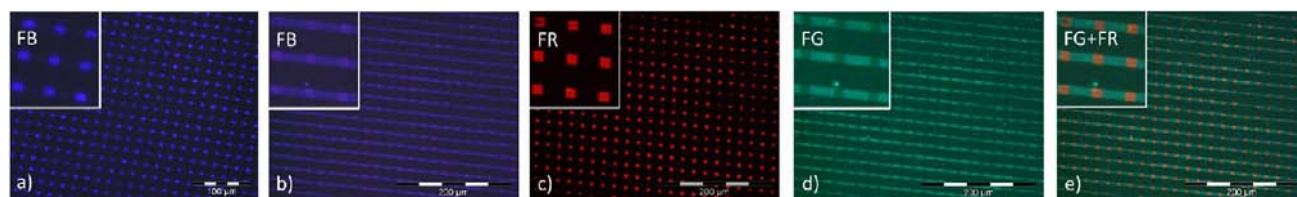
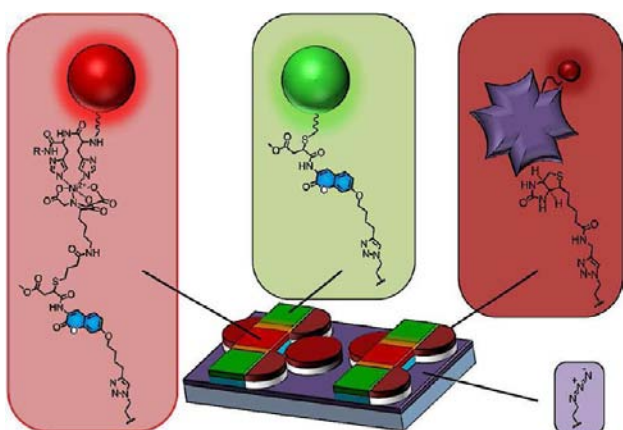


Figure 3. Fluorescence micrographs: (a) after cross-microcontact printing of lines of thiol-NTA perpendicular to the lines of **1** printed before further functionalization; (b–d) after overnight incubation of this substrate patterned with **1** and cross-microcontact printed thiol-NTA in $20 \mu\text{M}$ $\text{G}^{174\text{C}}\text{TFP}$ and subsequent incubation with $1 \mu\text{M}$ $\text{His}_6\text{-}^{14}\text{TagRFP-His}_6\text{:Ni}^{2+}$ (1:2) in PBS for 1 h; and (e) merged image of FR + FG. FB/FG/FR refer to blue (monitoring coumarin), green (monitoring TFP), and red (monitoring TagRFP) channels, respectively.

groups using reactive μ CP for further functionalization via an additional orthogonal 'click'-reaction with alkyne-modified biotin was investigated. In order to visualize the successful attachment of alkyne-modified biotin to the surface, the thus biotinylated substrate was incubated with a solution of $0.6 \mu\text{M}$ Cy5-labeled streptavidin (Cy5-SAv) and showed the successful specific binding of streptavidin on the biotin pattern (Figure S6).

In order to fabricate a triple protein pattern the biotin-SAv interaction was combined with the dual protein pattern introduced above. To achieve a triple protein array, such as that shown in the surface layout in Scheme 4, first the

Scheme 4. Schematic Representation of the Triple Protein Array^a



^aThe molecular structure of the NiNTA/His₆ complex represents one of the possible species formed upon interactions of a His₆-tag with a single NiNTA unit.

fluorogenic platform was prepared via reactive μ CP of lines of the fluorogenic coumarin **1** on the azide monolayer, followed by immobilization of thiol-NTA in squares using a cross- μ CP step. Subsequently, a dot-pattern of alkyne-biotin was cross-microcontact printed onto the remaining areas of azide groups on the substrate. After completion of these three printing steps, three different proteins were immobilized in consecutive steps: (a) ^{G174C}TFP via the direct Michael addition on the residual thiol-reactive coumarin tether (Figure 4c); (b) His₆-¹⁴TagRFP-His₆ via formation of a supramolecular complex with NTA ligands in the presence of Ni²⁺ ions (Figure 4b); and (c) Cy5-SAv via complexation with immobilized biotin (Figure 4d). As can be seen from the merged fluorescent images (Figure 4e), the formation of blue fluorescent lines (Figure 4a) reports the successful direct immobilization of thiol-NTA and of ^{G174C}TFP (Figure 4b,c) onto the fluorogenic tether. The incubation of the substrate with a solution of His₆-¹⁴TagRFP-His₆ in PBS resulted in selective, noncovalent immobilization of His₆-¹⁴TagRFP-His₆ solely on the NTA-functionalized cross-microcontact printed squares (Figure 4a,b). The successful immobilization of Cy5-SAv exclusively on the printed biotin dots is shown in Figure 4d.

The overlay of the fluorescent images (Figure 4e) of the three individual immobilizations of the three different proteins on the same surface proves the expected localization of the proteins on the doubly cross-microcontact printed array. With the above series we could show that: (a) we were able to specifically immobilize three different proteins on different

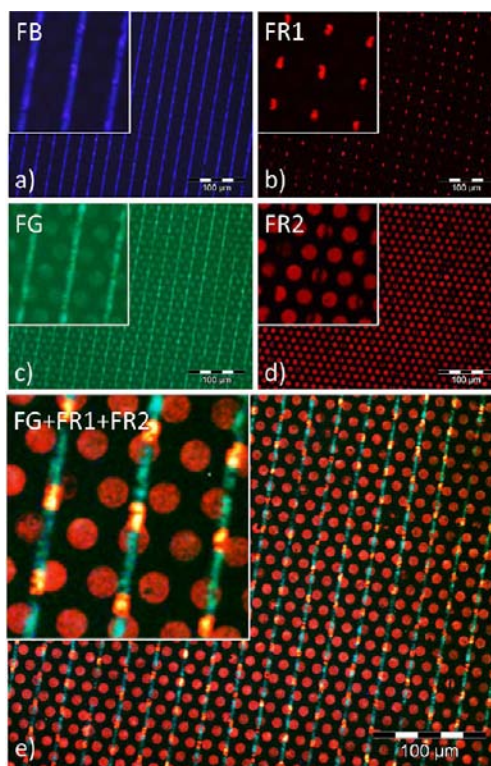


Figure 4. Fluorescence micrographs: (a–d) after cross-microcontact printed thiol-NTA on the fluorogenic coumarin, μ CP of alkyne-modified biotin and overnight incubation with ^{G174C}TFP solution, 1 h incubation with His₆-¹⁴TagRFP-His₆:Ni²⁺ (1:2), and 1 h incubation with Cy5-SAv; (e) merged image of FG, FR1 and FR2. FB/FG/FR (= FR1)/FR2 refer to blue (monitoring coumarin), green (monitoring TFP), red (monitoring TagRFP), and far-red (monitoring Cy5) channels, respectively.

parts of a pattern on one substrate; (b) the three methods of immobilization employed here are orthogonal and specific with regard to their respective surface functionalities; and (c) triple μ CP is a viable patterning technique for the fabrication of a triple protein array.

3. CONCLUSION

A fluorogenic platform was employed to selectively immobilize and fluorescently report on the immobilization of thiol-containing proteins and thiol-modified biomolecules. The fluorogenic platform proved to be an excellent tool to visualize the bond formation between biomolecule and surface, while the orthogonal immobilization at different parts of the patterned substrate could be visualized as well. The flexibility of this approach will allow for the fabrication of specific protein patterns and represents an important achievement on the way toward establishing surfaces with differentiated responsive functions. By themselves the chromophores contained in the fluorescent proteins that we have used in this study are not very complex but rather derive their fascinating properties from the tight interactions with the well-defined structure of the protein as a whole.²⁵ As such, fluorescent proteins present some of the most well-defined and easily modifiable systems known to date for the study and development of new, complex, and protein-compatible surface immobilization and patterning strategies. Interfaces such as those developed here can serve as additional tools for the study of cell–surface interactions in an orientationally controlled, multiprotein environment.

■ ASSOCIATED CONTENT

■ Supporting Information

Description of compounds; detailed printing procedures; procedures for protein modification and expression; Figures S1 (printed cysteine), S2 (cross-printed thiol-NTA), S3 (cross-printed thiol-NTA complexed with His₆-¹⁴TagRFP-His₆), S4 (cross-printed thiol-NTA followed by immobilization of G¹⁷⁴C TFP), S5 (cross-printed thiol-NTA followed by consecutive immobilization of His₆-¹⁴TagRFP-His₆ and G¹⁷⁴C TFP), S6 (printed alkyne-biotin followed by immobilization of Cy5-SAv), and S7 and S8. This material is available free of charge via the Internet at <http://pubs.acs.org>.

■ AUTHOR INFORMATION

Corresponding Author

v.subramaniam@utwente.nl; j.huskens@utwente.nl; p.jonkheijm@utwente.nl

Author Contributions

[§]These authors contributed equally.

Notes

The authors declare no competing financial interest.

■ ACKNOWLEDGMENTS

The fellowship of D.W. was cofunded by DAAD (D/08/46093). The work by C.N. and J.H. was supported by the Council for Chemical Sciences of The Netherlands Organization for Scientific Research (NWO-CW, Vici grant 700.58.443). The work by D.W. and P.J. was cofunded by a starting grant from the European Research Council (no. 259183 Sumoman). Also project P4.02 Superdices of the research program of the BioMedical Materials Institute, cofunded by the Dutch Ministry of Economic Affairs, Agriculture and Innovation is gratefully acknowledged by P.J.

■ REFERENCES

- (1) For reviews see for example: (a) Weinrich, D.; Jonkheijm, P.; Niemeyer, C. M.; Waldmann, H. *Angew. Chem., Int. Ed.* **2009**, *48*, 7744–51. (b) Kingsmore, S. F. *Nat. Rev. Drug Discovery* **2006**, *5*, 310–21. (c) Dufva, M.; Christensen, C. B. *Experts Rev. Proteomics* **2005**, *2*, 41–8. (d) Zhu, H.; Snyder, M. *Curr. Opin. Chem. Biol.* **2003**, *7*, 55–63.
- (2) For reviews see for example: (a) Chen, Y.-X.; Triola, G.; Waldmann, H. *Acc. Chem. Res.* **2011**, *44*, 762. (b) Wong, L. S.; Khan, F.; Micklefield, J. *Chem. Rev.* **2009**, *109*, 4025–53. (c) Jonkheijm, P.; Weinrich, D.; Schroeder, H.; Niemeyer, C. M.; Waldmann, H. *Angew. Chem., Int. Ed.* **2008**, *47*, 9618–47.
- (3) For a feature article see for example: Ganesan, R.; Kratz, K.; Lendlein, A. *J. Mater. Chem.* **2010**, *20*, 7322–31.
- (4) For examples see: (a) Soellner, M. B.; Dickson, K. A.; Nilsson, B. L.; Raines, R. T. *J. Am. Chem. Soc.* **2003**, *125*, 11790–1. (b) Watzke, A.; Koehn, M.; Gutierrez-Rodriguez, M.; Wacker, R.; Schroeder, H.; Breinbauer, R.; Kuhlmann, J.; Alexandrov, K.; Niemeyer, C. N.; Goody, R. S.; Waldmann, H. *Angew. Chem., Int. Ed.* **2006**, *45*, 1408–12. (c) de Araujo, A. D.; Palomo, J. M.; Cramer, J.; Kohn, M.; Schroeder, H.; Wacker, R.; Niemeyer, C.; Alexandrov, K.; Waldmann, H. *Angew. Chem., Int. Ed.* **2006**, *45*, 296–301. (d) Duckworth, B. P.; Xu, J. H.; Taton, T. A.; Guo, A.; Distefano, M. *Bioconjugate Chem.* **2006**, *17*, 967–74. (e) Lin, P. C.; Ueng, S. H.; Tseng, M. C.; Ko, J. L.; Huang, K. T.; Yu, S. C.; Adak, A. K.; Cheng, Y. J.; Lin, C. C. *Angew. Chem., Int. Ed.* **2006**, *45*, 4286–90. (f) Govindaraju, T.; Jonkheijm, P.; Gogolin, L.; Schroeder, H.; Becker, C. F. W.; Niemeyer, C. M.; Waldmann, H. *Chem. Commun.* **2008**, 3723–5. (g) Christman, K. L.; Broyer, R. M.; Tolstyka, Z. P.; Maynard, H. D. *J. Mater. Chem.* **2007**, *17*, 2021–7. (h) Lempens, E. H. E.; Helms, B. A.; Merckx, M.; Meijer, E. W. *ChemBioChem* **2009**, *10*, 658–62. (i) Zhang, K.; Diehl, M. R.;

Tirrell, D. A. *J. Am. Chem. Soc.* **2005**, *127*, 10136–7. (j) Weinrich, D.; Lin, P. C.; Jonkheijm, P.; Nguyen, U. T. T.; Schroeder, H.; Niemeyer, C. M.; Alexandrov, K.; Goody, R. S.; Waldmann, H. *Angew. Chem., Int. Ed.* **2010**, *49*, 1252–7. (k) Hodneland, C. D.; Lee, Y.-S.; Min, D.-H.; Mrksich, M. *Proc. Natl. Acad. Sci. U.S.A.* **2002**, *99*, 5048–52. (l) Kindermann, M.; George, N.; Johnsson, N.; Johnsson, K. *J. Am. Chem. Soc.* **2003**, *125*, 7810–1.

(5) For examples see: (a) Becker, C. F. W.; Wacker, R.; Bouschen, W.; Seidel, R.; Kolaric, B.; Lang, P.; Schroeder, H.; Mueller, O.; Niemeyer, C. M.; Spengler, B.; Goody, R. S.; Engelhard, M. *Angew. Chem., Int. Ed.* **2005**, *44*, 7635–9. (b) Hutschenreiter, S.; Tinazli, A.; Model, K.; Tampé, R. *EMBO J.* **2004**, *44*, 2488–97. (c) Kwon, Y.; Coleman, M. A.; Camarero, J. A. *Angew. Chem., Int. Ed.* **2006**, *45*, 1726–9. (d) Escalante, M.; Zhao, Y.; Ludden, M. J. W.; Vermeij, R.; Olsen, J. D.; Berenschot, E.; Hunter, C. N.; Huskens, J.; Subramaniam, V.; Otto, C. *J. Am. Chem. Soc.* **2008**, *130*, 8892–3. (e) Hwang, I.; Baek, K.; Jung, M.; Kim, Y.; Park, K. M.; Lee, D.-W.; Selvapalam, N.; Kim, K. *J. Am. Chem. Soc.* **2007**, *129*, 4170–1. (f) Young, J. F.; Nguyen, H. D.; Yang, L.; Huskens, J.; Jonkheijm, P.; Brunsveld, L. *ChemBioChem* **2010**, *11*, 180–3.

(6) Li, Y.; Niehaus, J. C.; Chen, Y.; Fuchs, H.; Studer, A.; Galla, H.-J.; Chi, L. *Soft Matter* **2011**, *7*, 861–3.

(7) (a) Vong, T.; ter Maat, J.; van Beek, T. A.; van Lagen, B.; Giesbers, M.; van Hest, J. C. M.; Zuilhof, H. *Langmuir* **2009**, *25*, 13952. (b) del Campo, A.; Boos, D.; Spiess, H. W.; Jonas, U. *Angew. Chem., Int. Ed.* **2005**, *44*, 4707. (c) Xu, H.; Hong, R.; Lu, T.; Uzun, O.; Rotello, V. M. *J. Am. Chem. Soc.* **2006**, *128*, 3162. (d) Sato, H.; Miura, Y.; Saito, N.; Kobayashi, K.; Takai, O. *Biomacromolecules* **2007**, *8*, 753. (e) Pritchard, D. J.; Morgan, H.; Cooper, J. M. *Angew. Chem., Int. Ed.* **1995**, *34*, 91–3. (f) Doh, J.; Irvine, D. J. *J. Am. Chem. Soc.* **2004**, *126*, 9170–1. (g) Holden, M. A.; Cremer, P. S. *J. Am. Chem. Soc.* **2003**, *125*, 8074–5. (h) Dubey, M.; Emoto, K.; Takahashi, H.; Castner, D. G.; Grainger, D. W. *Adv. Funct. Mater.* **2009**, *19*, 3046–55.

(8) (a) Rozkiewicz, D. I.; Brugman, W.; Kerkhoven, R. M.; Ravoo, B. J.; Reinhoudt, D. N. *J. Am. Chem. Soc.* **2007**, *129*, 11593. (b) Gupta, N.; Lin, B. F.; Campos, L. M.; Dimitriou, M. D.; Hikita, S. T.; Treat, N. D.; Tirrell, M. V.; Clegg, D. O.; Kramer, E. J.; Hawker, C. J. *Nat. Chem.* **2010**, *2*, 138–45.

(9) Christman, K. L.; Schnopf, E.; Broyer, R. M.; Li, R. C.; Chen, Y.; Maynard, H. D. *J. Am. Chem. Soc.* **2009**, *131*, 521–7.

(10) (a) Salaita, K.; Wang, Y. H.; Mirkin, C. A. *Nat. Nanotechnol.* **2007**, *2*, 145–55. (b) Paxton, W. F.; Spruell, J. M.; Stoddart, J. F. *J. Am. Chem. Soc.* **2009**, *131*, 6692–4. (c) Wu, C. C.; Reinhoudt, D. N.; Otto, C.; Subramaniam, V.; Velders, A. H. *Small* **2011**, *7*, 989–1002. (11) (a) Subramaniam, C.; Cengiz, N.; Saha, K.; Gevrek, T. N.; Yu, X.; Jeong, Y.; Bajaj, A.; Sanyal, A.; Rotello, V. M. *Adv. Mater.* **2011**, *23*, 3165–9. (b) Im, S. G.; Bong, K. W.; Kim, B.-S.; Baxamusa, S. H.; Hammond, P. T.; Doyle, P. S.; Gleason, K. K. *J. Am. Chem. Soc.* **2008**, *130*, 14424. (c) Slocik, J. M.; Beckel, E. R.; Jiang, H.; Enlow, J.; Zabinski, J. S.; Bunning, T. J.; Naik, R. R. *Adv. Mater.* **2006**, *18*, 2095.

(12) (a) Leibfarth, F. A.; Kang, M.; Ham, M.; Kim, J.; Campos, L. M.; Gupta, N.; Moon, B.; Hawker, C. J. *Nat. Chem.* **2010**, *2*, 207–12. (b) Spruell, J. M.; Sheriff, B. A.; Rozkiewicz, D. L.; Dichtel, W. R.; Rohde, R. D.; Reinhoudt, D. N.; Stoddart, J. F.; Heath, J. R. *Angew. Chem., Int. Ed.* **2008**, *47*, 9927–32. (c) Spruell, J. M.; Wolffs, M.; Leibfarth, F. A.; Stahl, B. C.; Heo, J.; Connal, L. A.; Hu, J.; Hawker, C. J. *J. Am. Chem. Soc.* **2011**, *133*, 16698–706. (d) Wendeln, C.; Rinnen, S.; Schulz, C.; Kaufmann, T.; Arlinghaus, H. F.; Ravoo, B. J. *Chem.—Eur. J.* **2012**, *18*, 5880–8. (e) Deng, X.; Friedmann, C.; Lahann, J. *Angew. Chem., Int. Ed.* **2011**, *50*, 6522–6.

(13) For reviews see for example: (a) Mager, M. D.; LaPointe, V.; Stevens, M. M. *Nat. Chem.* **2011**, *3*, 582–9. (b) Aida, T.; Meijer, E. W.; Stupp, S. I. *Science* **2012**, *335*, 813–7. (c) Fenske, T.; Korth, H.-G.; Mohr, A.; Schmuck, C. *Chem.—Eur. J.* **2012**, *18*, 738–55. (d) Uhlenheuer, D. A.; Petkau, K.; Brunsveld, L. *Chem. Soc. Rev.* **2010**, *39*, 2817–26.

(14) González-Campo, A.; Hsu, S.-H.; Puig, L.; Huskens, J.; Reinhoudt, D. N.; Velders, A. H. *J. Am. Chem. Soc.* **2010**, *132*, 11434–6.

- (15) For a recent review see: Wendeln, C.; Ravoo, B. J. *Langmuir* **2012**, *28*, 5527–38.
- (16) Nicosia, C.; Cabanas-Danés, J.; Jonkheijm, P.; Huskens, J. *ChemBioChem* **2012**, *13*, 778–82.
- (17) Newman, R. H.; Fosbrink, M. D.; Zhang, J. *Chem. Rev.* **2011**, *111*, 3614–66.
- (18) Balachander, N.; Sukenik, C. N. *Langmuir* **1990**, *6*, 1621–7.
- (19) Rozkiewicz, D. I.; Janczewski, D.; Verboom, W.; Ravoo, B. J.; Reinhoudt, D. N. *Angew. Chem., Int. Ed.* **2006**, *45*, 5292–6.
- (20) Yi, L.; Li, H.; Sun, L.; Liu, L.; Zhang, C.; Xi, Z. *Angew. Chem., Int. Ed.* **2009**, *48*, 4034–7.
- (21) Ai, H.; Henderson, J. N.; Remington, S. J.; Campbell, R. E. *Biochem. J.* **2006**, *400*, 531–40.
- (22) Sevier, C. S.; Kaiser, C. A. *Nat. Rev. Mol. Cell Biol* **2002**, *3*, 836–47.
- (23) Ellman, G. L. *Biochem. Biophys.* **1959**, *82*, 70–7.
- (24) Subach, O. M.; Malashkevich, V. N.; Zencheck, W. D.; Morozova, K. S.; Piatkevich, K. D.; Almo, S. C.; Verkhusha, V. V. *Chem. Biol.* **2010**, *17*, 333–41.
- (25) Dedecker, P.; De Schryver, F.; Hofkens, J. *J. Am. Chem. Soc.* **2012**, DOI: 10.1021/ja309768d.